Optics Letters

Dual-mode spatial index modulation for MIMO-OWC

Xin Zhong,[1] Chen Chen,[1,*] Yinan Zhao,[1] Min Liu,[1] Cuiwei He,[2] and Harald Haas[3]

[1]School of Microelectronics and Communication Engineering, Chongqing University, Chongqing 400044, China
[2]School of Information Science, Japan Advanced Institute of Science and Technology, Ishikawa 923-1211, Japan
[3]Technology Innovation Centre and Department of Electronic and Electrical Engineering, University of Strathclyde, G1 1RD Glasgow, UK
*c.chen@cqu.edu.cn

Received 18 October 2023; revised 28 November 2023; accepted 6 December 2023; posted 6 December 2023; published 4 January 2024

In this Letter, we propose and demonstrate a dual-mode spatial index modulation (DM-SIM) scheme for spectral efficiency enhancement of band-limited multiple-input multiple-output optical wireless communication (MIMO-OWC) systems. By performing dual-mode index modulation in the spatial domain, DM-SIM can transmit both spatial and constellation symbols. Since constellation design plays a vital role in the proposed DM-SIM scheme, we further propose three dual-mode constellation design approaches including phase rotation, amplitude scaling and joint phase rotation and amplitude scaling. Moreover, we also designed a differential log-likelihood ratio (LLR) detector for the proposed DM-SIM scheme. Experimental results show that the joint phase rotation and amplitude scaling approach can achieve a remarkable 3.2 dB signal-to-noise ratio (SNR) gain compared with the phase rotation approach in a 2×2 MIMO-OWC system applying DM-SIM.

https://doi.org/10.1364/OL.509658

Optical wireless communication (OWC) has been emerging as a pivotal and promising enabling technology for the sixth-generation (6G) of mobile networks in recent years, due to its many advantages, such as abundant and unregulated spectrum resources, low-cost front-ends, electromagnetic interference-free operation and high physical-layer security [1–3]. However, commercially available optical elements such as light-emitting diodes (LEDs), laser diodes (LDs) and photodiodes (PDs) are generally band limited. The usable modulation bandwidth of these optical elements is relatively small, especially for illumination LEDs which usually exhibit a −3 dB bandwidth of only several MHz [4]. Hence, it is of practical significance to enhance the spectral efficiency for a given modulation bandwidth so as to substantially boost the capacity of band-limited OWC systems.

As a capacity-enhancement technique in the spatial domain, multiple-input multiple-output (MIMO) transmission has been widely applied in band-limited OWC systems [5]. So far, three basic MIMO schemes including repetition coding (RC), spatial multiplexing (SMP), and spatial modulation (SM) have been introduced in MIMO-OWC systems [6]. Specifically, RC obtains diversity gain by using all the transmitters to transmit the same signal, SMP achieves multiplexing gain by employing different transmitters to transmit different signals, and SM is a digitized MIMO scheme which can transmit both spatial and constellation symbols [7–9]. Lately, various advanced MIMO schemes have been further reported in the literature. In [10], a generalized LED index modulation scheme has been proposed for 4×4 MIMO-OWC systems, where a complex time-domain orthogonal frequency division multiplexing (OFDM) signal is transmitted by using four LEDs. In [11], user-centric MIMO schemes including RC/SMP switching, adaptive SMP and RC-aided adaptive SMP have been proposed by exploiting users' spatial positions as a new degree of diversity.

Moreover, generalized MIMO schemes including generalized SM and generalized SMP have been further proposed for MIMO-OWC systems in [12–14]. Compared with SM which only activates one transmitter to transmit signal, generalized MIMO schemes can activate multiple transmitters to transmit signals. Nevertheless, only a subset of all the transmitters can be activated to transmit signals in order to transmit additional spatial bits, and hence there exist idle transmitters which are not used to transmit signals, which inevitably limits the achievable capacity of band-limited MIMO-OWC systems. On the other hand, if all the transmitters are activated to transmit signals, e.g., RC and SMP, no additional spatial bits can be transmitted. Therefore, it remains to be an open problem how to transmit additional spatial bits while utilizing all the transmitters to transmit signals in band-limited MIMO-OWC systems.

Aiming to address the above-mentioned problem, in this Letter, we, for the first time, propose a novel dual-mode spatial index modulation (DM-SIM) scheme for spectral efficiency enhancement of band-limited MIMO-OWC systems. By designing two distinguishable constellation sets, dual-mode index modulation can be successfully performed in the spatial domain, and hence the proposed DM-SIM scheme can utilize all the transmitters to transmit both spatial and constellation symbols. To efficiently implement DM-SIM, we further propose three dual-mode constellation design approaches and a differential log-likelihood ratio (LLR) detector. Proof-of-concept experiments are conducted to evaluate the performance of MIMO-OWC systems applying the proposed DM-SIM scheme.

Without a loss of generality, a 2×2 MIMO-OWC system is considered to introduce the principle of the proposed DM-SIM scheme, and DM-SIM is applicable to a general MIMO-OWC system with a larger MIMO size. The schematic diagram of an OFDM-based MIMO-OWC system using the proposed DM-SIM scheme is depicted in Fig. 1, where $N_t = N_r = 2$. As we can see, the input bits are first partitioned into three parts, namely, spatial bit b_s, constellation bits $b_{c,A}$ for mode A, and constellation

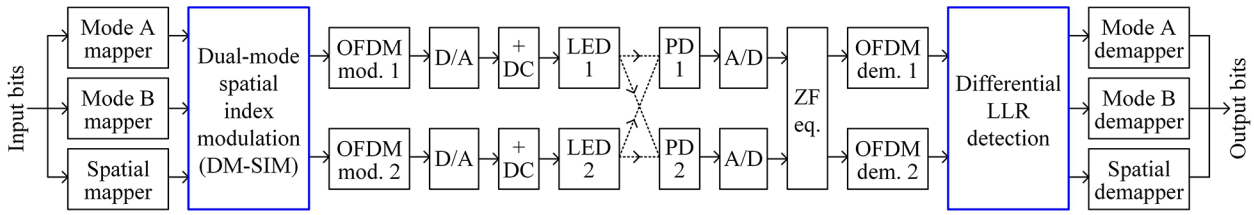

Fig. 1. Schematic diagram of an OFDM-based MIMO-OWC system using the proposed DM-SIM scheme with differential LLR detection for $N_t = N_r = 2$. Mod., modulation; dem. demodulation; eq., equalization.

Table 1. DM-SIM Mapping Table for $N_t = 2$

b_s	s_1	s_2	$\mathbf{s}$	$\mathbf{x}$
0	1	2	[1, 2]	$[c_\alpha^{\mathrm{A}}, c_\beta^{\mathrm{B}}]$
1	2	1	[2, 1]	$[c_\beta^{\mathrm{B}}, c_\alpha^{\mathrm{A}}]$

bits $b_{\mathrm{c,B}}$ for mode B. The distinguishable constellation sets for constellation mappers A and B are, respectively, denoted by $\mathcal{M}_{\mathrm{A}}$ and $\mathcal{M}_{\mathrm{B}}$ with $\mathcal{M}_{\mathrm{A}} \cap \mathcal{M}_{\mathrm{B}} = \varnothing$, and the sizes of $\mathcal{M}_{\mathrm{A}}$ and $\mathcal{M}_{\mathrm{B}}$ are represented by M_{A} and M_{B}, respectively. Then, b_{s} is sent into the spatial mapper to generate the spatial index vector $\mathbf{s} = [s_1, s_2]$, while $b_{\mathrm{c,A}}$ and $b_{\mathrm{c,B}}$ are fed into mode A mapper and mode B mapper to generate constellation symbols c_α^{A} and c_β^{B}, respectively, with $\alpha = 1, 2, \ldots, M_{\mathrm{A}}$ and $\beta = 1, 2, \ldots, M_{\mathrm{B}}$. After that, DM-SIM is performed with respect to the two spatial channels for a given subcarrier slot to generate the transmit signal vector $\mathbf{x} = [x_1, x_2]$. The DM-SIM mapping table for $N_t = 2$ is given in Table 1. Specifically, one spatial bit can be transmitted in the 2×2 MIMO-OWC system applying DM-SIM. If the spatial bit is zero at the given subcarrier slot, the first spatial channel (i.e., LED 1) is selected to transmit constellation symbol c_α^{A} from $\mathcal{M}_{\mathrm{A}}$, while the second spatial channel (i.e., LED 2) is selected to transmit constellation symbol c_β^{B} from $\mathcal{M}_{\mathrm{B}}$. On the contrary, if the spatial bit is one at the given subcarrier slot, the first and second spatial channels are assumed to transmit c_β^{B} and c_α^{A}, respectively.

Subsequently, parallel OFDM modulation is executed and the OFDM modulation includes the procedures of inverse fast Fourier transform (IFFT) with Hermitian symmetry and parallel-to-serial (P/S) conversion. After digital-to-analog (D/A) conversion and adding direct current (DC) bias, two parallel real-valued nonnegative electrical signals are obtained, which are finally used to drive LED 1 and LED 2 to generate the output optical signals. After a free-space transmission, the optical signals are captured by two photo-detectors (PDs), and the detected analog signals are converted into digital signals *via* an analog-to-digital (D/A) conversion. Then, a zero-force equalization is carried out for MIMO demultiplexing [14]. The equalization signals undergo parallel OFDM demodulation, which includes serial-to-parallel (S/P) conversion, fast Fourier transform (FFT), and frequency-domain equalization (FDE), and hence, the estimate of the transmit signal vector $\mathbf{x}$, i.e., $\hat{\mathbf{x}} = [\hat{x}_1, \hat{x}_2]$, can be obtained.

Finally, a differential LLR detector is designed to perform DM-SIM detection. At a given subcarrier slot, the LLR value of the i-th ($i = 1, 2$) spatial channel can be calculated by [15]

$$\lambda_i = \ln\left(\sum_{\alpha=1}^{M_{\mathrm{A}}} \exp\left(-\frac{1}{P_n}\left|x_i - c_\alpha^{\mathrm{A}}\right|^2\right)\right) - \ln\left(\sum_{\beta=1}^{M_{\mathrm{B}}} \exp\left(-\frac{1}{P_n}\left|x_i - c_\beta^{\mathrm{B}}\right|^2\right)\right), \tag{1}$$

where P_n denotes the noise power at the given subcarrier slot in the frequency domain and $c_\alpha^{\mathrm{A}} \in \mathcal{M}_{\mathrm{A}}$, $c_\beta^{\mathrm{B}} \in \mathcal{M}_{\mathrm{B}}$. It should be noted that P_n might be different at different subcarrier slots due to the low-pass frequency response of the band-limited MIMO-OWC system. Letting $\Delta\lambda = \lambda_1 - \lambda_2$ denote the difference of the LLR values, the spatial index vector $\mathbf{s}$ can be estimated as follows:

$$\hat{\mathbf{s}} = \begin{cases} [1, 2], & \text{if } \Delta\lambda > 0 \\ [2, 1], & \text{if } \Delta\lambda \le 0 \end{cases}. \tag{2}$$

According to $\hat{\mathbf{s}}$, the estimated constellation symbols $\hat{c}_\alpha^{\mathrm{A}}$ and $\hat{c}_\beta^{\mathrm{B}}$ can be extracted from $\hat{\mathbf{x}}$. Consequently, the output bits can be obtained by demapping $\hat{\mathbf{s}}$, $\hat{c}_\alpha^{\mathrm{A}}$ and $\hat{c}_\beta^{\mathrm{B}}$.

Considering a general $N_r \times N_t$ MIMO-OWC system applying the proposed DM-SIM scheme where k out of totally N_t spatial channels are selected to transmit constellation symbols from $\mathcal{M}_{\mathrm{A}}$ while the rest $N_t - k$ spatial channels transmit constellation symbols from $\mathcal{M}_{\mathrm{B}}$, the overall spectral efficiency is given by

$$\eta = \underbrace{\left\lfloor \log_2(C(N_t, k)) \right\rfloor}_{\text{spatial symbol}} + \underbrace{k \log_2 M_{\mathrm{A}} + (N - k) \log_2 M_{\mathrm{B}}}_{\text{constellation symbols}}, \tag{3}$$

where $\lfloor \cdot \rfloor$ represents the floor operator which outputs an integer smaller or equal to its input value and $C(N_t, k)$ denotes the binomial coefficient. It can be seen from Eq. (3) that the first term is contributed by the spatial symbol while the second and third terms are contributed by the dual-mode constellation symbols.

As discussed above, the overall performance of DM-SIM-based MIMO-OWC systems largely depends on the adopted two distinguishable constellation sets $\mathcal{M}_{\mathrm{A}}$ and $\mathcal{M}_{\mathrm{B}}$. To this end, we further propose three dual-mode constellation design approaches by exploiting the phase and/or amplitude of a base constellation. Without loss of generality, we here take $M_{\mathrm{A}} = M_{\mathrm{B}} = 4$ as an example. Figures 2(a), (b), and (c) illustrate the dual-mode constellation design approaches based on phase rotation, amplitude scaling and joint phase rotation and amplitude scaling, respectively. For the phase rotation approach, as shown in Fig. 2(a), the standard 4-ary quadrature amplitude modulation (4-QAM) constellation plotted in blue squares represents the constellation set $\mathcal{M}_{\mathrm{A}}$ for mode A, and the constellation set $\mathcal{M}_{\mathrm{B}}$ for mode B as depicted in red circles can be obtained by rotating $\mathcal{M}_{\mathrm{A}}$ as follows:

$$\mathcal{M}_{\mathrm{B}} = \mathcal{M}_{\mathrm{A}} \exp(j\theta), \tag{4}$$

where θ is the rotated angle. For the amplitude scaling approach, as illustrated in Fig. 2(b), the constellation set $\mathcal{M}_{\mathrm{B}}$ can be achieved from $\mathcal{M}_{\mathrm{A}}$ *via* amplitude scaling as follows:

$$\mathcal{M}_{\mathrm{B}} = \mu \mathcal{M}_{\mathrm{A}}, \tag{5}$$

where $\mu = d_2/d_1$ is the amplitude scaling factor, with d_1 and d_2 denoting the radii of the circles corresponding to $\mathcal{M}_{\mathrm{A}}$ and $\mathcal{M}_{\mathrm{B}}$,

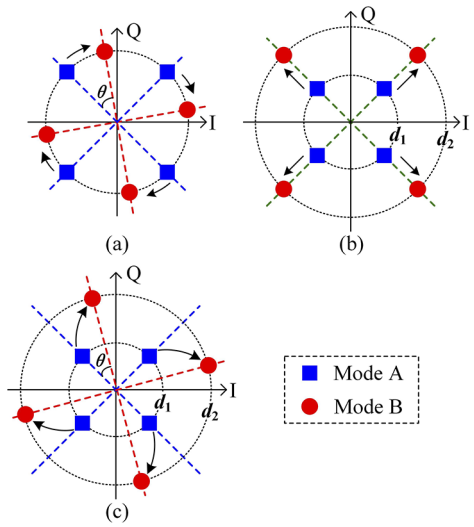

Fig. 2. Constellation design: (a) phase rotation, (b) amplitude scaling, and (c) joint phase rotation and amplitude scaling.

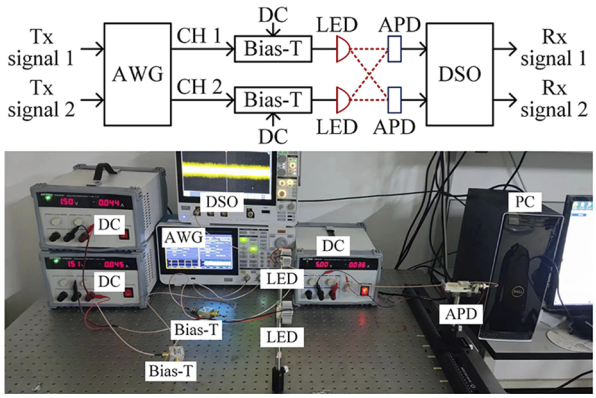

Fig. 3. Experimental setup of a 2×2 MIMO-OWC system using infrared LEDs.

respectively. For the joint phase rotation and amplitude scaling approach, as can be seen from Fig. 2(c), the constellation set $\mathcal{M}_B$ is generated from $\mathcal{M}_A$ through both phase rotation and amplitude scaling, which can be expressed by

$$\mathcal{M}_B = \mu \mathcal{M}_A \exp(j\theta). \tag{6}$$

It can be observed from Figs. 2(a), (b), and (c) that the rotated angle θ and/or the amplitude scaling factor μ might be optimized to minimize the overall bit error rate (BER) performance of the MIMO-OWC system applying the proposed DM-SIM scheme.

To evaluate the performance of DM-SIM, proof-of-concept experiments are conducted by a 2×2 MIMO-OWC setup. Figure 3 depicts the experimental setup of the 2×2 MIMO-OWC system using infrared LEDs. As we can see, the transmitted signals are first generated offline by MATLAB, which are then sent to a two-channel arbitrary waveform generator (AWG, Tektronix AFG31102) with a sampling rate of 25 MSa/s. Then, a DC bias current of 50 mA is combined with each of the two AWG output signals *via* a bias tee. Subsequently, the two combined signals are used to drive two infrared LEDs which both have a field of view (FOV) of 60°. At the receiver side, an avalanche photodiode (APD, Hamamatsu C12702-12) is utilized to detect the light signals at two receiver positions. The detected electrical signals are captured by a digital storage oscilloscope (DSO,Tektronix MDO32) with a sampling rate of 250 MSa/s, and the resultant digital signals are further processed offline in MATLAB. In the experimental setup, the spacing between two infrared LEDs is 30 cm, the spacing between two receiver positions is 10 cm, and the transmission distance is 45 cm. Moreover, the size of IFFT/FFT in OFDM modulation is 128 and a total of 32 subcarriers are used to carry valid data. As a result, the effective signal bandwidth is 25×32/128 = 6.25 MHz. When applying the proposed DM-SIM scheme in the 2×2 MIMO-OWC system with $N_t = 2$, $k = 1$, and $M_A = M_B = 4$, according to Eq. (3), the overall spectral efficiency is 5 bits/s/Hz, and hence the data rate is 5×6.25 = 31.25 Mbits/s.

We first evaluate the three constellation design approaches in the DM-SIM-based 2×2 MIMO-OWC system. Figure 4(a) shows the experimental BER versus rotated angle for the phase rotation approach with an AWG input peak-to-peak voltage (Vpp) of 3 V. It can be found that the BER first gradually decreases and then increases when the rotated angle is increased from 30° to 60°, and the minimum BER of 6.9×10^{-4} is achieved with an optimal rotated angle of 45°. The insets in Fig. 4(a) depict the corresponding received constellations for rotated angles of 35°, 45°, and 55°. As we can clearly observe, the optimal rotated angle of 45° can maximize the minimum Euclidean distance between the constellation points in two different modes, and therefore the lowest BER can be obtained. Figure 4(b) shows the experimental BER versus amplitude scaling factor for the amplitude scaling approach with Vpp = 3 V. It is also evident that the BER is first gradually decreased and then increased with the amplitude scaling factor increasing from 1 to 2.2, and the BER reaches the minimum value of 5.7×10^{-4} with an optimal amplitude scaling factor of 2. The corresponding received constellations for amplitude scaling factors of 1.5, 2, and 2.25 are given in the insets in Fig. 4(b). Similarly, the optimal amplitude scaling factor of 2 can ensure that the minimum Euclidean distance between the constellation points in two different modes will have a maximum value to minimize the BER. Figure 4(c) presents the contour plot of BER versus the rotated angle and amplitude scaling factor for the joint phase rotation and amplitude scaling approach with Vpp = 3 V. Evidently, there exits an optimal combination of rotated angle and amplitude scaling factor, i.e., (45°, 1.75), that can result in a minimum BER of 7.8×10^{-5}. The inset in Fig. 4(c) shows the received constellation for a rotated angle of 45° and an amplitude scaling factor of 1.75. It can be concluded from Figs. 4(a), (b), and (c) that it is feasible to optimize the rotated angle and/or the amplitude scaling factor so as to achieve a minimum BER for the DM-SIM-based 2×2 MIMO-OWC system.

We further investigate the relationship between BER and average received SNR for the three dual-mode constellation design approaches in the DM-SIM-based 2×2 MIMO-OWC system, where the three average received SNR values of 7, 12.7, and 15.6 dB are considered, which are corresponding to three Vpp values of 1, 2, and 3 V, respectively. Figure 5 presents the experimental BER versus average received SNR for DM-SIM with three dual-mode constellation design approaches and the conventional MIMO scheme. For DM-SIM schemes, optimization is performed for each average received SNR value. For conventional MIMO, 4-QAM and 8-QAM are adopted in two spatial channels to achieve the same spectral efficiency of 5 bits/s/Hz. As we can see, the phase rotation approach obtains the worst BER

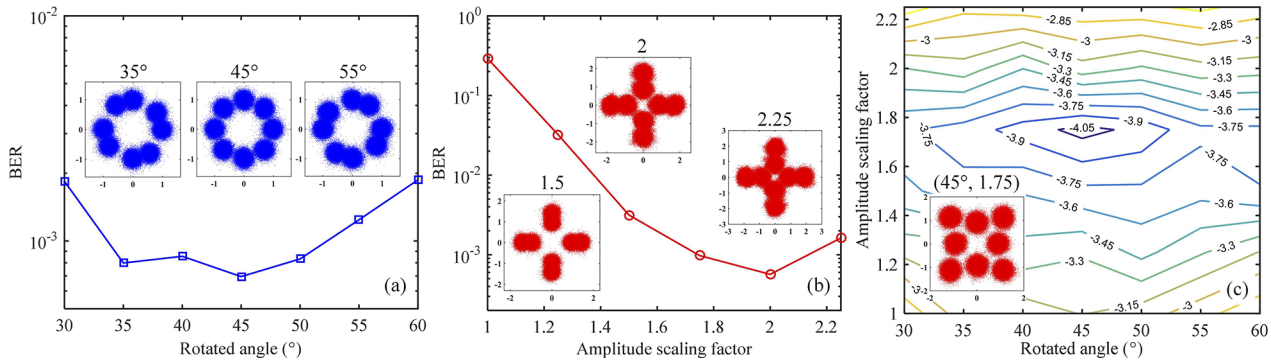

Fig. 4. Experimental results: (a) BER versus rotated angle, (b) BER versus amplitude scaling factor, and (c) contour plot of $\log_{10}$BER versus rotated angle and amplitude scaling factor.

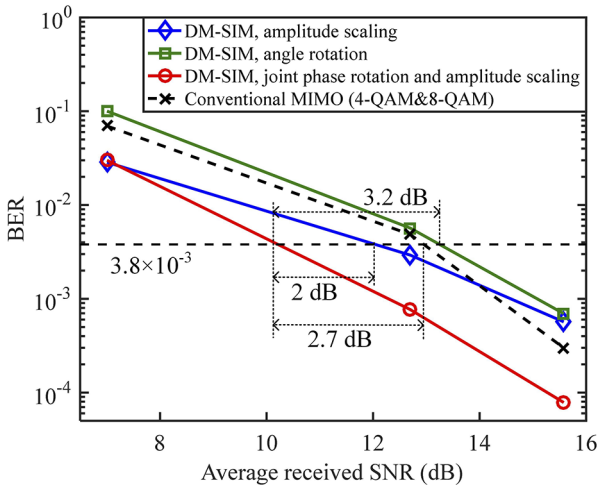

Fig. 5. Experimental BER versus average received SNR for different schemes.

performance, which requires an average received SNR of 13.3 dB to reach the 7% forward error correction (FEC) coding limit of BER = 3.8×10^{-3}. Moreover, the amplitude scaling approach performs slightly better than the phase rotation approach, and the required SNR for the amplitude scaling approach to reach BER = 3.8×10^{-3} is 12.1 dB. It is exciting to see that the joint phase rotation and amplitude scaling approach achieves the best BER performance, which reaches BER = 3.8×10^{-3} with an average received SNR of 10.1 dB. As a result, the joint phase rotation and amplitude scaling approach outperforms the phase rotation and amplitude scaling approaches by remarkable SNR gains of 3.2 dB and 2 dB, respectively. Furthermore, the required average received SNR for the conventional MIMO scheme to reach BER = 3.8×10^{-3} is 12.8 dB. Hence, a 2.7-dB SNR gain can be achieved by DM-SIM with joint phase rotation and amplitude scaling in comparison to the conventional MIMO scheme.

In this Letter, we have proposed and experimentally demonstrated a novel DM-SIM scheme for MIMO-OWC systems. To enable DM-SIM in MIMO-OWC systems, three dual-mode constellation design approaches have been further proposed. Moreover, a differential LLR detector has also been designed to realize DM-SIM detection. It is shown by the experimental results that the joint phase rotation and amplitude scaling approach performs the best among all the three dual-mode constellation design approaches. Therefore, DM-SIM with joint phase rotation and amplitude scaling based dual-mode constellation design can be a promising candidate for high-speed MIMO-OWC systems.

Funding. National Natural Science Foundation of China (62271091, 61901065); Natural Science Foundation of Chongqing (cstc2021jcyj-msxmX0480).

Disclosures. The authors declare no conflicts of interest.

Data availability. Data underlying the results presented in this paper are not publicly available at this time but may be obtained from the authors upon reasonable request.

REFERENCES

1. N. Chi, Y. Zhou, Y. Wei, *et al.*, IEEE Veh. Technol. Mag. **15**, 93 (2020).
2. Z. Wei, Z. Wang, J. Zhang, *et al.*, Prog. Quantum Electron. **83**, 100398 (2022).
3. M. D. Soltani, H. Kazemi, E. Sarbazi, *et al.*, IEEE Trans. Commun. **71**, 1024 (2023).
4. S. Rajagopal, R. D. Roberts, and S.-K. Lim, IEEE Commun. Mag. **50**, 72 (2012).
5. L. Zeng, D. C. O'Brien, H. Le Minh, *et al.*, IEEE J. Select. Areas Commun. **27**, 1654 (2009).
6. T. Fath and H. Haas, IEEE Trans. Commun. **61**, 733 (2013).
7. R. Mesleh, H. Elgala, and H. Haas, J. Opt. Commun. Netw. **3**, 234 (2011).
8. A. Burton, H. Minh, Z. Ghassemlooy, *et al.*, IEEE Photonics Technol. Lett. **26**, 945 (2014).
9. J. Lian and M. Brandt-Pearce, J. Lightwave Technol. **35**, 5024 (2017).
10. A. Yesilkaya, E. Basar, F. Miramirkhani, *et al.*, IEEE Trans. Commun. **65**, 3429 (2017).
11. C. Chen, H. Yang, P. Du, *et al.*, IEEE Syst. J. **14**, 3202 (2020).
12. S. Alaka, T. L. Narasimhan, and A. Chockalingam, in Proc. IEEE Global Commun. Conf. (GLOBECOM) (2015), p. 1.
13. F. Wang, F. Yang, and J. Song, Opt. Express **28**, 21202 (2020).
14. C. Chen, X. Zhong, S. Fu, *et al.*, J. Lightwave Technol. **39**, 6063 (2021).
15. T. Mao, Z. Wang, Q. Wang, *et al.*, IEEE Access **5**, 50 (2017).